THERMAL ENDURANCE OF PHOTOACTIVE WATERBORNE POLYURETHANE/CARBON QUANTUM DOTS MATERIALS

Lucas Dall Agnol[1]*, Fernanda T. G. Dias[2] and Otávio Bianchi[1,3]

1 – Postgraduate Program in Materials Science and Engineering (PGMAT), University of Caxias do Sul (UCS), Caxias do Sul, RS, Brazil
agnol.lucasdall@gmail.com and otavio.bianchi@gmail.com
2 – Postgraduate Program in Technology and Materials Engineering (PPG-TEM), Federal Institute of Education, Science and Technology of Rio Grande do Sul (IFRS), Campus Feliz, RS, Brazil
3 – Department of Materials Engineering (DEMAT), Federal University of Rio Grande do Sul (UFRGS), Porto Alegre, RS, Brazil

Abstract: This work was developed due to the need for searching alternatives to increase the thermal resistance of water-based polyurethane (WPU) photoactive films for the surface coating area. The effect of incorporating only 1.0 wt% carbon quantum dots (CQDs) on the thermal degradation behavior of the WPU was studied using thermodynamic and kinetic parameters. The incorporation of nanoparticles to the WPU increased the initial polymer degradation temperature from 252°C to 270°C, due to reactions between active hydrogens in CQDs surface and –NCO groups of WPU. Kinetic and thermodynamic parameters extracted from the thermal degradation of WPU/CQDs nanocomposite allowed predicting its thermal endurance. An improvement of ~11% in the WPU endurance time was detected after incorporating 1.0 wt% CQDs into the polymer. The nanocomposite reported here can be applied in photoactive coating systems with good thermal stability.

Keywords: *waterborne polyurethane; carbon quantum dots; photoactive coating; thermal stability; thermal endurance.*

Introduction

Photoluminescent materials have received great attention in applications as biosensors due to their distinct advantages over solution-based probes, including excellent stability; ease of transport, storage and recycling; non-invasive nature and tunable shape and size. In recent years, carbon quantum dots (CQDs) have shown exceptional potential in developing these applications [1]. CQDs are generally small carbon nanoparticles with high chemical stability, high photoluminescence, low-cost synthesis, and resistance to photobleaching [2, 3]. The surface hydroxy and carboxylic groups of these materials provide excellent solubility in water and organic solvents but hinder their deposition as thin films by conventional methods (vacuum filtration, electrophoretic deposition, or centrifugal coating).

Moreover, in environments where they are insoluble, these nanostructures lose their photoactivity in the solid-state [1]. Using a polymer matrix as support can facilitate the application of CQDs and prevent their photoluminescence loss, also providing mechanical resistance and catalytic stability to the final material. Waterborne polyurethane (WPU) emerges as an option for CQDs support due to its excellent mechanical, chemical, and adhesion properties and low emission of organic volatiles [4]. Also, the excellent transparency of polyurethane makes it an ideal matrix for producing suitable fluorescent materials [5]. WPU is also soluble in water, contributing to the distribution of CQDs in the matrix and preserving its photoluminescence activity. During synthesis,

the polyurethane chains can be chemically linked at the surface of the embedded CQDs to form a slightly cross-linked network structure, leading to improved nanocomposite properties [5]. The resulting nanocomposites can be applied to different surfaces, such as wood, metal, glass, or other plastics. When coating a surface, the WPU forms an impermeable barrier between the outer and the coated surface [6], but it has low thermal stability. Thus, the current work aims to evaluate the effect of CQDs on WPU thermal stability, using the prediction of the thermal endurance corresponding to 5% of materials degradation as the main comparative parameter.

Experimental

Synthesis of CQDs

The CQDs were synthesized by microwave-assisted pyrolysis of an aqueous solution of citric acid (CA; 98.5% purity, Sigma Aldrich) and ethylenediamine (EDA; ≥ 99.5% purity, Sigma Aldrich) (1:1 molar ratio). The mixture was irradiated for 6 min in a domestic microwave oven (650 W). The resulting red-brown solid was dissolved and dialyzed against pure water through a dialysis membrane (MWCO of 100) for 3 days. After dialysis, the obtained solution was lyophilized to yield powdered CQDs.

Synthesis of WPU/CQDs nanocomposites

At first, polycarbonate diol (PCD, 2000 g/mol; UBE Corporation Europe), hexamethylene diisocyanate (HDI, ≥99% purity, Sigma Aldrich) and 2,2-bis(hydroxymethyl)propionic acid (DMPA, 98% purity, Sigma Aldrich) were added into a dry four-necked flask equipped with a mechanical stirrer, oil-bath, condenser, dropping funnel and nitrogen inlet. The mixture was stirred (180 rpm) for 6 h at 80 ºC under nitrogen atmosphere. Whenever necessary, acetone was added to decrease the viscosity of the reaction mixture. After the temperature was reduced to 45 °C, triethylamine (TEA, ≥99.5% purity, Sigma Aldrich) was incorporated and homogenized for 45 min. Finally, the prepolymer was dispersed in an aqueous solution of CQDs under vigorously stirring (1100 rpm) for 30 min. The stoichiometric ratio of HDI/PCD/DMPA/TEA was 3.5:1:1:1.2. Two films named WPU and WPU/CQDs were prepared using 0 and 1.0 wt% of CQDs, respectively. The films were prepared by pouring the dispersions on a Teflon substrate and drying at 45 ºC for 72 h. The film thickness was fixed at approximately 30 μm.

Chemical structure and photoluminescence

Fourier transform infrared (FTIR) spectra were recorded on a Perkin Elmer Impact 400 spectrometer ($4000-400$ cm^{-1}, 64 scans, and 4 cm^{-1} resolution) using attenuated total reflectance mode (ATR, diamond at 45º). The ultraviolet-visible (UV–vis) absorption spectra were obtained in a spectrophotometer (Evolution 60S Thermo Scientific) from 200–800 nm at a wavelength step of 1 nm. The photoluminescence emission (PL) spectra were recorded on a Perkin Elmer LS 45 spectrometer using an excitation wavelength at 360 nm. The size distribution of CQDs was determined at 25 °C using dynamic light scattering (DLS; Delsa™ Nano Series, Beckman Coulter) equipped with a laser diode (30 mW, $\lambda = 658$ nm) and light source at a 165° dispersion angle.

Thermal endurance properties

Thermal properties were evaluated by thermogravimetric analysis (TGA) in a TGA-50 Shimadzu equipment, from 25 °C to 800 °C at four heating rates (5, 10, 20, and 40 °C.min^{-1}) under a nitrogen atmosphere (50 mL.min^{-1}). By treating TGA curves through the Friedman (FR) method, it was possible to calculate the kinetic triplet, which is composed of activation energy (E_a), pre-exponential factor (A), and kinetic function $f(a)$ – reaction mechanism parameters.

The correlation between kinetic and thermodynamic parameters of the investigated process results from the combination of Arrhenius and Eyring laws by Eq 1 [7]:

$$A = \left(\frac{e\chi k_B T_p}{h}\right) \exp\left(\frac{\Delta S^*}{R}\right) \quad\quad (1)$$

Where A is the pre-exponential factor obtained from the FR method; e=2.7183 is the Neper number; k_B is the Boltzmann constant; χ is the transition factor, unity for monomolecular reactions; h is the Plank constant, and T_p is the peak temperature of DTG curve. The entropy variation in thermal degradation could be determined by Eq 2:

$$\Delta S^* = R \ln\left(\frac{Ah}{e\chi k_B T_p}\right) \quad\quad (2)$$

The Gibbs free energy variation (ΔG^*) of the complex activation was obtained through the well-known thermodynamic theories [$\Delta H^* = E_a - R\,T_p$], and [$\Delta G^* = \Delta H^* - T_p\,\Delta S^*$]. The variables activation energy (ΔH^*), activation entropy (ΔS^*), and free activation energy (ΔG^*) were calculated at $T=T_{5\%}$ degradation.

The thermal endurance was calculated using the Arrhenius activation energy generated by TGA decomposition data according to ASTM E1877-15 by Eq 3:

$$\log[t_f] = E_\alpha/[(2.303\,R\,T) + \log[E_\alpha/(R\,\beta)] - \alpha] \quad\quad (3)$$

Where t_f is the estimated thermal endurance (thermal life) taken as the failure criterion (min) and T is the temperature (K) at 5% of thermal degradation.

Results and Discussion

The synthesized CQDs showed a well-dispersed size distribution, with a mean diameter of 10.9 ± 8.2 nm, determined by DLS. The CQDs photoluminescence behavior is shown in Fig. 1a. The CQDs exhibited an optical absorption peak in the UV region with maximum absorbance at 350 nm, attributed to n−π* transition of C=O and C−N groups from the nanomaterial surface [5]. The CQDs solution had light yellow and intense fluorescent blue colors under visible and UV (at excitation of 360 nm) lights, respectively (see the inset in Fig. 1a). A strong PL emission peak at 440 nm was observed for an excitation wavelength at 360 nm. When 1.0 wt% CQDs were incorporated into the WPU matrix, the nanocomposite showed good transparency and strong photoluminescence (Fig. 1b).
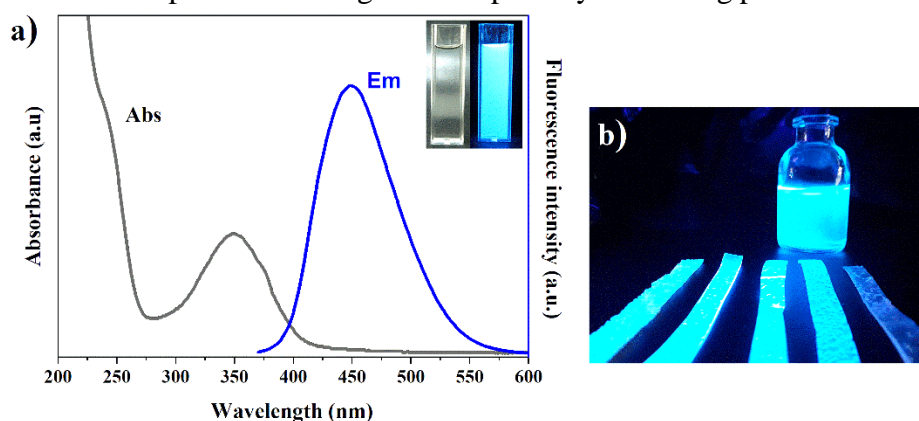

Figure 1 − (a) UV-vis and fluorescence spectra of the CQDs [inset-photographs of CQDs aqueous solution under daylight (left) and 365 nm UV light (right)] and (b) photographs of the WPU/CQDs solution (upper) and solid WPU/CQDs films (bottom) under UV light (365 nm)

The WPU and WPU/CQDs showed strong absorption bands at 3360–3420 cm^{-1} (N–H stretching vibration), 2955 cm^{-1} (CH$_2$ and CH$_3$ stretching vibration), 1738 cm^{-1} and 1637 cm^{-1} (C=O stretching vibrations), 1540 cm^{-1} (N–H bending vibration of NCO), and 1244 cm^{-1} (C–N stretching vibration) attributed to the WPU [Fig. 2 (a)] [4]. The C=O stretching region can be decomposed into three subcomponents, comprising hydrogen-bonded (~1670 cm^{-1}), nonhydrogen-bonded (at 1698 cm^{-}

[1]), and free carbonyl (at 1719 cm^{-1}) contributions, respectively [Fig. 2(b)] [4]. It is noticeable that the relative intensities of the different peaks have changed with the introduction of CQDs.
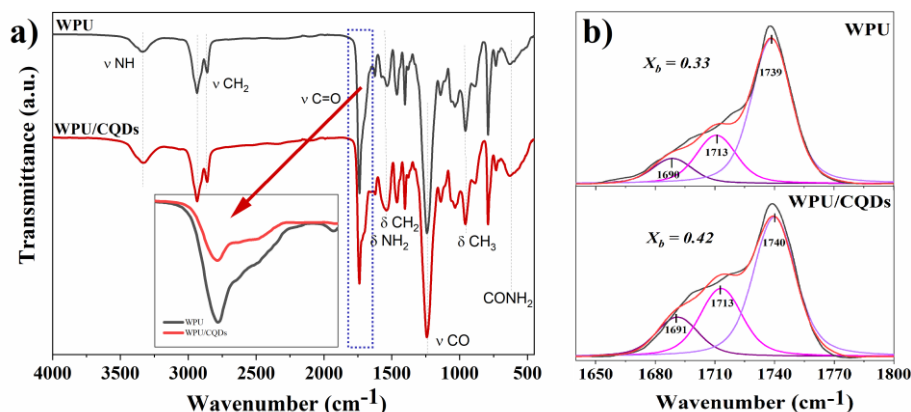

Figure 2 – (a) FTIR spectra and (b) curve fitting results at C=O stretching region for WPU and WPU/CQDs films

To analyze the areas of the three deconvolved band regions: $[X_o = A_{1690}/(A_{1690} + A_{1711} + A_{1740})]$; $[X_d = A_{1711}/(A_{1690} + A_{1711} + A_{1740})]$, and $[X_b = (X_0 + X_d)]$; where X_b, X_o, and X_d represent the hydrogen bonding relative degree and the percentages of ordered and disordered hydrogen bonds, respectively. As a result: WPU ($X_b = 0.113$; $X_o = 0.221$ and, $X_d = 0.335$) and WPU/CQDs ($X_b = 0.146$; $X_o = 0.271$ and, $X_d = 0.418$). The results of these particular areas confirm the influence of CQDs presence on the microdomain structure of the nanocomposite. The multifunctionality of CQDs, especially their chemical crosslinking character, increases the hydrogen bonding degree and phase separation in the WPU-based system. As a consequence, occurs a reduction of segmental chain motion [5].

The initial thermal degradation (α=5 wt%) temperature (T_5 wt%) increased from 252 °C to 270 °C, with the addition of 1 wt% CQDs [Fig. 3(a)]. The specific interactions between WPU and CQDs restrict the mobility of polymer chains. The behavior of E_a *versus* degradation mass loss curves [Fig. 3(b)] denotes a process composed of three degradation steps, being the first one within $0 \leq \alpha \leq 0.2$, the second at $0.2 \leq \alpha \leq 0.8$, and the third at $0.8 \leq \alpha \leq 1$. The mean values of E_α and A were: WPU ($E_\alpha = 124.8$ kJ.mol^{-1}; $A = 8.48$ s[-1]) and WPU/CQDs ($E_\alpha = 133.6$ kJ.mol^{-1}; $A = 9.01$ s[-1]). The first degradation stage corresponds to the urethane bonds decomposition. The second step corresponds to the decomposition of the soft segment and other products resulting from the first stage. In the third degradation step, the carbonic fraction is consumed until there are CQDs. The results presented in Fig. 3(b) suggest an increase in the thermal stability on the first and second degradation steps [8].

The negative values for entropy change (ΔS^*) correspond to a more ordered system and suggest that degradation reaction is slower than usual (Table 2). The positive values for ΔH^* indicate that the decomposition was endothermic in nature (see also Fig. 3). The positive values of ΔG^* supported the non-spontaneous degradation behaviors of the films, justifying the need for an external heat supply. The WPU and WPU/CQDs materials exhibited thermodynamic values relatively close to each other. However, for WPU/CQDs, more energy is needed for the degradation of the nanocomposite. By the thermodynamic triplet of the 1° DTG peak, it is observed that the nanoparticles slow down the degradation of the WPU rigid phase since they interact through hydrogen bonds with the urethane groups. This effect is less significant for the WPU flexible phase (2° DTG peak). Also, the thermal endurance calculation allowed the investigation of materials' thermal resistance over an extended period. While for the WPU material, a thermal endurance time of 0.018 h was predicted, the nanocomposite WPU/CQDs showed a value of 2.094 h. Hence, overall the kinetic-thermodynamic investigation was significantly helpful in elucidating the thermal stability of the films.
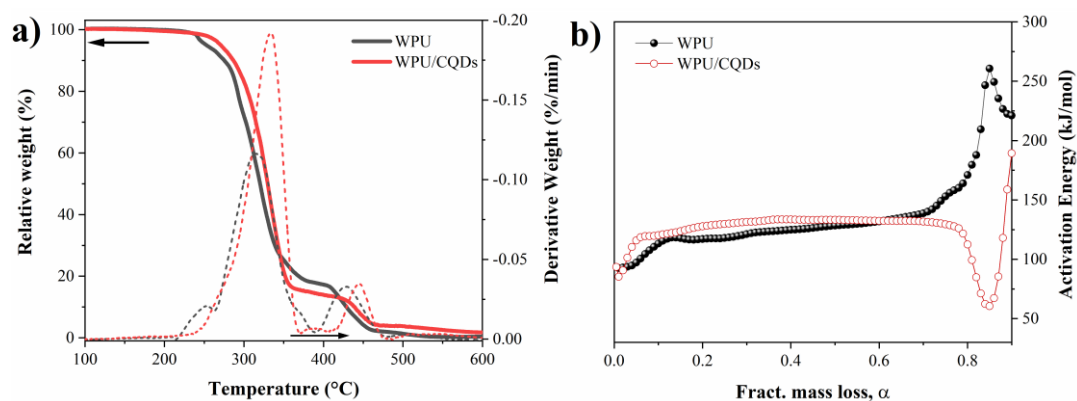
Figure 3 – (a) thermogravimetric and differential thermogravimetric curves and (b) dependence of the activation energy *vs*. conversion degree for WPU and WPU/CQDs films

Table 2 – Thermodynamic parameters and endurance time for WPU and WPU/CQDs materials

Samples	1° DTG peak			2° DTG peak			Endurance time
	ΔH*	*ΔS**	*ΔG**	*ΔH**	*ΔS**	*ΔG**	t$_f$ (5%) (h)
WPU	120.44	-188.14	231.32	152.27	-169.54	271.10	0.018
WPU/CQDs	128.34	-183.74	240.00	121.70	-190.15	258.85	2.094

Conclusions

Here, a WPU/CQDs nanocomposite with strong luminescence was produced by *in situ* polymerization. The incorporation of 1.0 wt% CQDs to WPU caused an increase of almost 7% in the initial degradation temperature compared to neat WPU material. Furthermore, the nanocomposite presented a hydrogen bonding degree increased. The WPU and WPU/CQDs materials showed thermal endurance times of 0.018 h and 2.094 h, respectively, for a temperature corresponding to 5% degradation. The WPU/CQDs reported here could be promising in applications such as photoactive coatings with good thermal properties.

Acknowledgments

References

1. P.R. Sreenath; S. Singh; M.S. Satyanarayana; P. Das; K. Dinesh Kumar *Polymer* 2017, *112*, 189.

2. M.M. Al Awak; P. Wang; S. Wang; Y. Tang; Y.P. Sun; L. Yang *RSC Adv.* 2017, *7*, 30177.

3. Z.M. Markovic; M. Kovacova; P. Humpolicek; M.D. Budimir; *et al*., *Photodiagnosis Photodyn. Ther.* 2019, *26*, 342.

4. Q. Li; L. Guo; T. Qiu; J. Ye; L. He; X. Li; X. Tuo *Prog. Org. Coat.* 2018, *122*, 19.

5. J. Bai; W. Ren; Y. Wang; X. Li; C. Zhang; Z. Li; Z. Xie *High Perform. Polym.* 2020, *32*, 857.

6. H.L. Friedman *J. Polym. Sci., Part C: Polym. Symp.* 2007, *6*, 183.

7. B. Boonchom; S. Puttawong *Physica B Condensed Matter.* 2010, *405*, 2350.

8. P.A. Ourique; F.G. Ornaghi; H.L. Ornaghi; C.H. Wanke; O. Bianchi *J. Therm. Anal. Calorim.* 2019, *137*, 1969.